Construction and Building Materials 174 (2018) 466–473

Contents lists available at ScienceDirect

Construction and Building Materials

journal homepage: www.elsevier.com/locate/conbuildmat

Pull-out creep mechanism of synthetic macro fibres under a sustained load

Adewumi John Babafemi [a], Anton du Plessis [b], William Peter Boshoff [a,*]

[a] Unit for Construction Materials, Department of Civil Engineering, Stellenbosch University, South Africa
[b] CT Scanner Facility, Stellenbosch University, South Africa

HIGHLIGHTS

- Polypropylene and modified olefin macro fibres both show significant pull-out creep.
- This pull-out creep is a combination of fibre lengthening and end-slip.
- Embossed fibres has less pull-out creep than non-embossed fibres.
- X-ray CT scans show that the end-slip is far less than the fibre lengthening.

ARTICLE INFO

Article history:
Received 2 July 2017
Received in revised form 17 April 2018
Accepted 18 April 2018
Available online 24 April 2018

Keywords:
Fibre pull-out
Fibre creep
Synthetic macro fibre
Macro-synthetic fibre reinforced concrete
Time-dependent fibre pull-out

ABSTRACT

The creep of cracked fibre reinforced concrete is still being investigated for incorporation into design guidelines. While the mechanism responsible for the time-dependent crack opening of steel fibre reinforced concrete has been associated with the fibre pull-out, a combination of pull-out creep and fibre creep have been reported for macro-synthetic fibre reinforced concrete. However, these phenomena are yet to be fully understood. In macro-synthetic fibre reinforced concrete, two possibilities exist: simultaneous occurrence of pull-out creep and fibre lengthening occurring within the matrix under sustained loading, or pull-out creep followed by fibre lengthening due to creep. This study investigates these phenomena. Single synthetic macro fibres were embedded into 50 mm cube cement-mortar samples and subjected to 50% of the average maximum pull-out load obtained from the single fibre pull-out tests. All tests were conducted in a controlled climate room. X-ray computed tomography (CT) images of samples were taken at different time intervals to assess the phenomena responsible for the increased crack widening in macro-synthetic fibre reinforced concrete. The results obtained have shown that the phenomena associated with the increased crack widening of cracked macro-synthetic fibre reinforced concrete are a simultaneous interplay of fibre pull-out and lengthening within the matrix. It is significant to note that fibre lengthening is a prominent mechanism.

1. Introduction

As the use of short, discrete fibres in concrete applications continues to see increased usage in the construction industry, research is also being intensified to fully understand the behaviour of fibre reinforced concrete (FRC), and the mechanisms associated with observed responses under different test conditions [1,2]. Fundamentally, fibres toughen concrete, thereby controlling crack propagation by bridging crack plane. Furthermore, the effectiveness of the fibres in crack control is hinged on several factors bordering around the concrete matrix, the fibre type (including geometry and orientation), and the fibre/matrix interface.

The failure mechanism in a cracked FRC element is primarily a result of the fibres pulling out or fracturing under load [3,4]. The failure mechanism is, however, dependent on the type of fibre and the fibre/matrix bond strength among others. With steel fibres, complete fibre pull-out is typically experienced [5–8]. The rupturing of steel fibre has been reported in some cases to be due to snubbing effect [9] and crimped configuration [10]. In an autoclave reactive powder concrete, images from the SEM photos revealed that steel fibre rupture occurred due to improved hydration reactions and the tobermorite gel congestion in the fibre-matrix interface [11]. Steel fibre rupture was also reported in an alkali-activated slag cements (AASC) based composites [12]. The rupture

* Corresponding author at: Civil Engineering Department, Stellenbosch University, Private Bag X1, Stellenbosch 7602, South Africa.
E-mail address: bboshoff@sun.ac.za (W.P. Boshoff).

https://doi.org/10.1016/j.conbuildmat.2018.04.148
0950-0618/

was attributed to its high drying shrinkage values, different microstructure and fresh state properties. Furthermore, Khabaz [13] observed the rupture of corrugated steel fibre due to higher embedment length. The phenomena associated with the pull-out of steel fibres have been described by several authors [10,14]. On the other hand, for synthetic macro fibres, which are known to have a poor bond with cement/concrete matrix due to their hydrophobic nature, the failure mechanism is typically by complete fibre pull-out [15]. However, fibre rupture has been reported for synthetic micro fibres where a chemical bond is present [16].

Several studies have assessed the performance of macro-synthetic FRC, usually, in comparison to steel fibres [17–22]. Others have discussed the single fibre pull-out mechanism of synthetic fibres from cement matrix in a quasi-static test [15,23–29]. Since structures are subjected to time-dependent loading, creep becomes a necessary factor for consideration when dealing with FRC. When synthetic macro fibres are used to reinforce concrete elements, significant creep caused could be expected [30].

Some studies have been conducted at the single fibre level to understand the mechanisms responsible for the time-dependent crack opening of cracked synthetic FRC elements [30–32]. The two primary mechanisms have been identified as pull-out creep and fibre creep. The study by Boshoff et al. [31] revealed that the creep of polyvinyl alcohol (PVA), a micro synthetic fibre, had no significant contribution to the time-dependent crack opening of the cement-based composite tested. However, Babafemi & Boshoff [30] and Vrijdaghs et al. [32] have reported that the creep of macro synthetic fibre significantly contributes to the time-dependent crack opening of FRC elements under sustained loadings. There is a significant difference between the creep of crack synthetic fibre reinforced concrete compared to the use of steel fibres. As steel is known to have little to no creep, the main mechanism is fibre slipping/pull-out while with synthetic fibres, the main mechanism is the fibres lengthening combined with fibre pull-out [2,15,30].

Though these failure mechanisms (pull-out creep and fibre creep) are known, the creep failure of macro synthetic FRC is not yet fully understood. Some phenomena could be associated with the pull-out creep mechanism. The first is the fibre pull-out creep upon the application of sustained load followed by the creep of the pulled out portion of the fibre. Secondly, a simultaneous pull-out creep and fibre creep could occur within the matrix with the fibre also creeping outside the matrix. Still, fibre creep could occur upon the application of sustained load followed by pull-out creep and then creep of pulled out fibre. Whichever the case, the time-dependent lengthening is a function of the low elastic modulus of the fibre, while the pull-out creep could be a function of the fibre material, geometrical properties, surface configuration and shape if the matrix composition is kept constant.

In this study, an investigation of the phenomena associated with the time-dependent fibre pull-out of synthetic macro fibre from cement matrix has been carried out. The study has been conducted using three types of synthetic macro fibres with a different configuration and geometrical properties. Instantaneous single fibre pull-out tests were performed to determine the average maximum pull-out load. After that, pull-out creep tests of single fibres embedded in mortar matrix subjected to a fraction of the average maximum pull-out load were quantified. To gain further insight into the phenomena associated with the failure mechanisms, samples subjected to creep loads were subjected to X-ray computed tomography (CT) scans to relate the pull-out creep of the fibre from the external surface to the internal creep (within the matrix). The review of micro-CT scanning for applications in the materials sciences [33] and an example of porosity analysis in concretes is given in Du Plessis et al. [34].

2. Experimental programme

2.1. Materials and concrete mix

The concrete materials and proportion used for the preparation of the concrete mix are shown in Table 1. The cement, CEM I 52.5N, had a relative density (RD) of 3.14, while the crushed stone and natural sand, locally known as Greywacke stone and fine Malmesbury sand had relative densities of 2.72 and 2.62, respectively. The fine Malmesbury sand, passing through a 2.36 mm sieve, has a fineness modulus of 1.14, while the coarse aggregate passed through a 9 mm sieve size but retained on 4.75 mm. Since all tests for the investigation were performed at the single fibre level, no fibre was added to the concrete mixture. However, the mixture was designed as though fibres were to be added, and hence a superplasticiser, Chryso® Fluid Optima 206, supplied by Chryso, South Africa, was added to enhance workability.

After the preparation of the fresh concrete mix, the slump value was measured using Abrams cone according to the requirement of EN 12350-2 [35]. A slump value of 145 mm was obtained.

2.2. Synthetic macro fibres

Three types of synthetic macro fibres were used. The fibres and their properties are shown in Fig. 1 and Table 2. The equivalent diameter (d_{eq}) was calculated following the procedure outlined in EN 14889-2 [36]. Fibres 1 and 3 have continuously embossed surface configuration while Fibre 3 is crimped. A handful of each fibre type was added to the concrete mixture during mixing to simulate actual fibre condition as the aggregates in the mix damages the surface of the fibre during mixing [37]. This pre-damaging of the fibres during mixing was done for 3 min.

All fibres were added to the concrete mixtures at the same time for uniformity in mixing condition and time. The fibres were later handpicked during sieving (4.75 mm sieve) of the concrete mixture to obtain mortar paste. After that, the fibres were washed and marked to the required embedment length.

2.3. Sample preparation

Samples were prepared for two sets of tests: quasi-static fibre pull-out and fibre pull-out creep. The fresh concrete mixture was sieved to eliminate the stones using a 4.75 mm sieve to obtain only the mortar paste. Sieving off the stones aided the easy insertion of the flexible fibres into the paste. The samples for the quasi-static fibre pull-out test have dimensions of $40 \times 40 \times 100$ mm^3. The samples were obtained by using a wooden separator in a 100 mm cube size mould as shown in Fig. 2a). The paste was then cast into the moulds and vibrated using a vibrating table. On the other hand, the samples for the pull-out creep test were prepared by casting the mortar paste into 50 mm cube steel moulds. Pre-damaged fibres, which had already been marked to 20 mm, were then manually inserted into the midpoint of the surface area of each sample. The moulds were gently vibrated to ensure the closure of voids created during the insertion of the fibres. The fibres were adjusted manually and visibly checked to ensure they were perpendicular to the surface of the matrix. Cast samples are shown in Fig. 2b). All test samples were demoulded after 24 h and cured in water at a temperature of 25 °C until testing.

Quasi-static fibre pull-out tests were conducted on the 28-day, while the pull-out creep tests commenced on the 29-day after the samples were left in the climate-controlled room for 24 h. Ten numbers of 100 mm cube samples were also cast and tested for compressive strength. The compressive strength tests were performed according to the requirement of EN 12390-3 [38].

2.4. Single fibre pull-out test

Except for different sample size and fibre clamping device used in this study, the single fibre pull-out test setup has been previously reported in Babafemi & Boshoff [15]. A clamp was fabricated with two flat steel plates (40×40 mm^2) to grip the fibre. A 2 kN capacity load cell was attached to the setup to measure the applied load. The fibre portion protruding from the matrix was clamped as close as possible to the surface to eliminate any elastic elongation of the free length. Pull-out displacement during the test was measured using two 50 mm linear variable displacement transducers (LVDT), which were supported by polyvinyl alcohol (PVC) strip attached to the test setup as shown in Fig. 3. The pull-out tests were

Table 1
Mix composition and proportion of concrete materials.

Material type	Volume (kg/m^3)
Cement (CEM I 52.5 N)	370
Stone (Greywacke = 9 mm)	891
Sand (fine Malmesbury)	891
Water	204
Superplasticizer (0.8% by wt of binder)	2.96

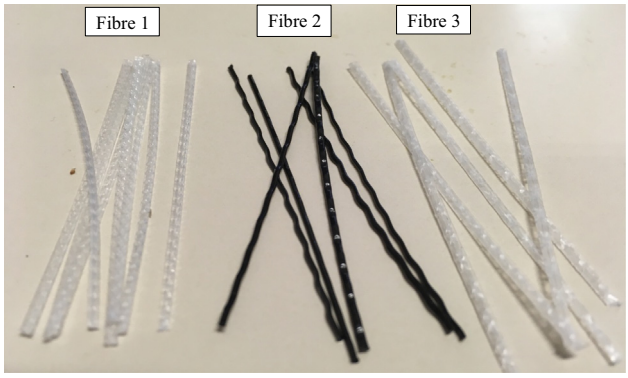

Fig. 1. Synthetic macro fibres.

performed at a displacement rate of 0.2 mm/s. Adequate care was taken to ensure that no force was applied to the fibre that could have led to debonding or pull-out before the commencement of the test. In cases where such was suspected, the samples were discarded. It should noted that using a $40 \times 40 \times 100\ mm^3$ specimen allowed for the clamping of the test specimen well below the embedded fibre to prevent any clamping pressure on the fibre.

2.5. Pull-out creep test setup

The pull-out creep of the three fibres was quantified under a sustained load equivalent to 50% of their respective average maximum pull-out loads. The tests were performed in a climate-controlled room at a temperature of 23 °C ± 0.5 and relative humidity of 65% ± 0.5. The samples were held in position by a hollow 100 mm cube square steel section shown in Fig. 4a). A centre groove, measuring 25 mm (width) × 75 mm (length), was cut open on one side of the steel section as shown in Fig. 4b). On the opposite side of the opening, the steel section was drilled to accommodate a 10 mm threaded bar connecting it to the supporting frame as shown in Fig. 5a). The time-dependent pull-out displacement (pull-out creep) was measured using two LVDTs attached to the fibre clamp as shown in Fig. 5b). The pull-out creep displacement acquisition was initiated using the HBM Spider8 Electronic Measuring System before the sustained loads for each fibre type was carefully applied. Care was taken to prevent dynamic vibration after the load application.

2.6. Pull-out creep mechanism using CT scan images

One sample each of Fibre 1 and Fibre 2 was subjected to the same sustained load, and pull-out creep measured as described in Section 2.5 to investigate the mechanisms occurring during the pull-out creep tests. The samples were unloaded and taken for CT scans at several intervals. Micro-CT scans were performed at the Stellenbosch CT facility [39]. The unloading-scanning-reloading cycle was repeated to visualise the pull-out mechanism occurring within the concrete and to correlate the internal displacement with that measured using the LVDTs. The choice of the 50 mm cube sample size was to prevent possible modification of the test sample in a bid to fit the sample size requirement for the CT scan. Too large samples do not allow sufficiently high resolution and too small samples would affect the pull-out behaviour. Scan settings included 160 kV and 160 μA for X-ray generation with 0.5 mm copper beam filtration. The voxel size was set to 30 μm to provide best possible resolution of the fibre pull-out.

3. Test results and discussion

This section presents the results of all tests performed and the discussion ensuing from the results. The concrete (with coarse aggregate) mixture was tested for compressive strength after 28 days as previously mentioned. Nine 100 mm cube samples were tested. The mean compressive strength is 35.9 MPa with a coefficient of variation of 5.8%.

3.1. Single fibre pull-out test results

The results of the single fibre pull-out tests for the different synthetic macro fibres is shown in Fig. 6(a–c), while the average performance for the purpose of comparison is shown in Fig. 6d). It should be noted that the averages, Fig. 6d) is shown on a different vertical scale. All the fibres were pre-marked before they were embedded 20 mm into the matrix. Some fibres, however, appear to have embedment length beyond 20 mm, particularly for Fibre 1 test set. The slight vibration of the moulds to close the voids created during the manual insertion of the fibres may have been the cause. The slight increases in the embedment length beyond 20 mm led to a corresponding increase in the pull-out load as observed in Fig. 6a). The corresponding increase in pull-out load with increase in the embedment agrees with literature [15,37].

As characteristic of FRC, the pull-out behaviour of each fibre type shows significant scatter within each test set. All Fibres 1 and 3 all pulled out completely from the matrix with a wave-like pattern in the post-peak region. The wave-like pattern demonstrated during pull-out in the post-peak region is the result of the surface deformation (embossment) created on the fibres. The surface deformation aids bonding with the matrix and enhancing resistance to pull-out load, consequently, increasing the friction between the fibre and the matrix. However, with Fibre 2, all test samples failed by fracturing during pull-out as seen in Fig. 6b). It should be noted that they ruptured at a load less than the specified strength (641 N). This lower load can be ascribed to the damage done to the fibre during mixing [37]. Fibre fracture occurred near the sample surface rather than at the clamp. Furthermore, in comparison with Fibres 1 and 3, it would be observed that pull-out response up to the maximum load showed a more non-linear response, as seen in Fig. 6d). This behaviour is believed to be linked to the fibre material, tensile strength and low elastic modulus as shown in Table 2. The fibres produced from modified olefin performed better than the polypropylene fibre.

The mean responses of the fibres shown in Fig. 6d) reveal that Fibre 1 performs better than the other two fibres with an average maximum pull-out load of 174 N. Though Fibres 1 and 3 are of the same material, tensile strength and elastic modulus, it should be reiterated that Fibre 1 has a larger diameter (0.85 mm) compared to Fibre 3 (0.74 mm). This result shows that the equivalent diameter of the fibre does influence the pull-out response.

3.2. Pull-out creep test results

After obtaining the mean maximum pull-out load for each fibre type, the time-dependent pull-out responses of the fibres were investigated at 50% load level of the mean maximum pull-out load as described in Section 2.5. The average pull-out creep of each fibre type is shown in Fig. 7a) for a duration of 30 days. Only one sample

Table 2
Properties of synthetic macro fibres.

Fibre type	Fibre material	Fibre length (mm)	d_{eq} (mm)	Specific gravity	Tensile strength (MPa)	Modulus of elasticity (GPa)	Cross-section	Fibre shape
EPC BarChip 54 (Fibre 1)	Modified Olefin	54	0.85	0.91	640	10	Irregular	Embossed surface
Geotex 500 Series (Fibre 2)	Polypropylene	50	0.71	0.91	405	4.3	Round	Crimped
EPC BarChip 48 (Fibre 3)	Modified Olefin	48	0.74	0.91	640	10	Irregular	Embossed surface

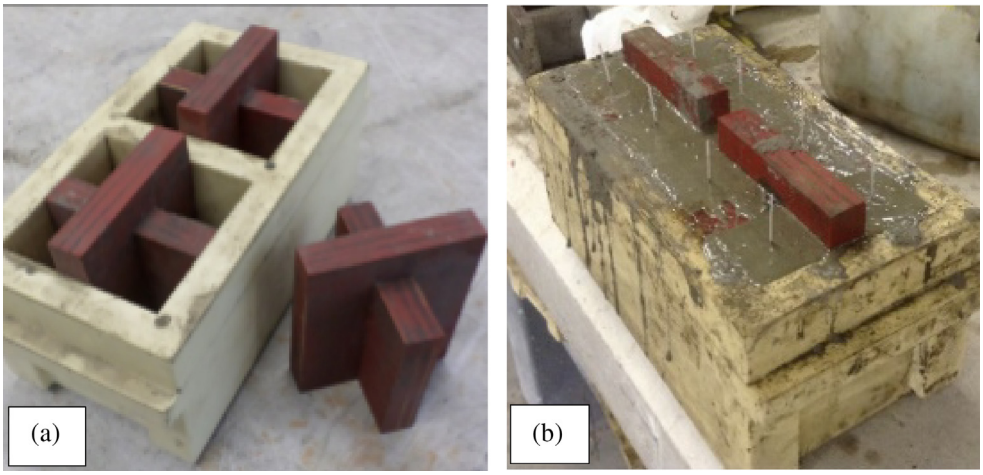

Fig. 2. (a) Moulds showing wooden separators (b) cast samples showing inserted fibres.

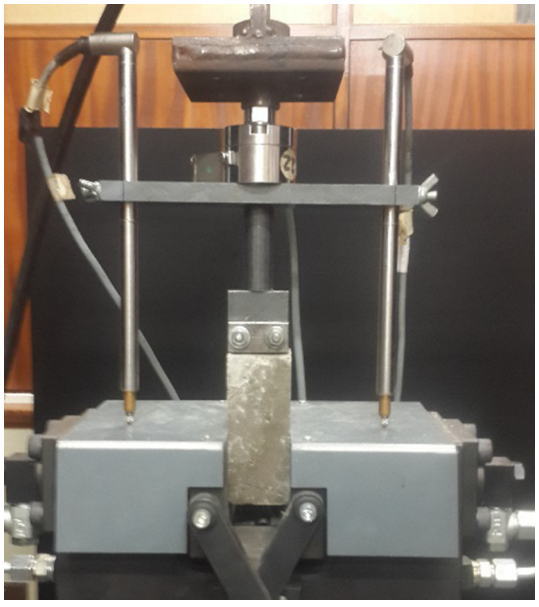

Fig. 3. Single fibre pull-out test setup.

for each fibre has been tested and reported here. However, it is acknowledged that great variability can be obtained even within the same sample set as characteristic with fibre reinforced composites.

As soon as the creep loads were applied, an instantaneous pull-out displacement (δ_{inst}) for all three fibre types occurred. The δ_{inst} seems to depend on the fibre type and properties, with Fibre 1 showing the least δ_{inst} followed by Fibres 2 and 3. Furthermore, the pull-out creep of the fibres in Fig. 7 continued to increase for both Fibre 1 and 3 at a decreasing rate. At the end of the test period (30 days) under sustained loads, Fibre 3 pulled out by 1.1 mm, while the pull-out creep for Fibre 1 is 0.9 mm. However, for Fibre 2, the pull-out creep continues to increase until the fibre pulled out completely from the matrix after 22 days.

Comparing the pull-out creep performance of fibres tested in this study to that previously reported in Babafemi & Boshoff [30] reveals that fibre property influences the pull-out creep response. The polypropylene macro fibre tested in Babafemi & Boshoff [30] pulled out in less than four days at the same 50% load level, while the embossed polypropylene fibre tested by Vrijdaghs et al. [32] pulled out completely in less than three days. It should be noted that irrespective of the fibre type, the total time-dependent pull-out displacement is a combination of the fibre creep and the

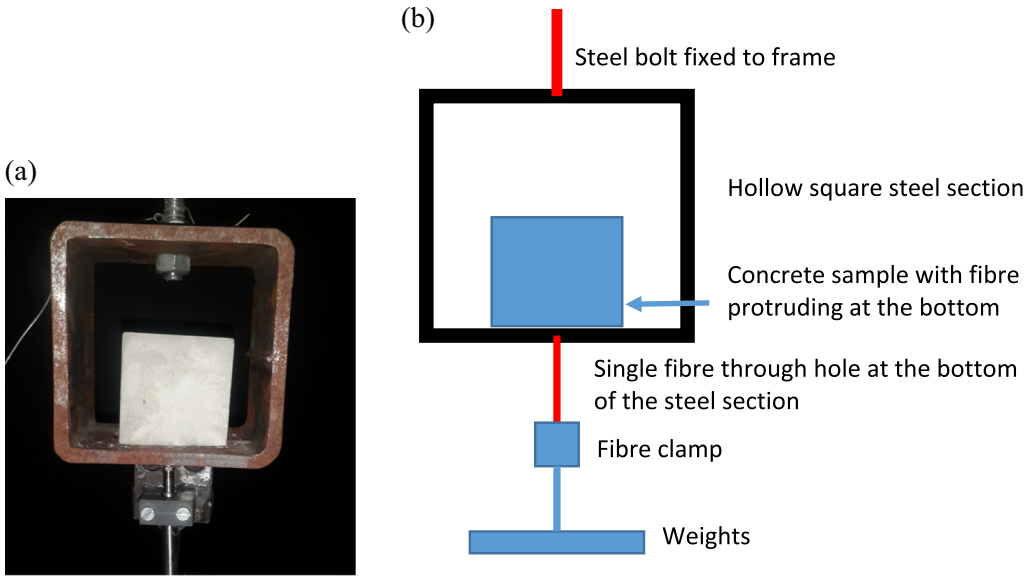

Fig. 4. (a) Sample placed in position on steel section for the pull-out creep test (b) diagram of the setup.

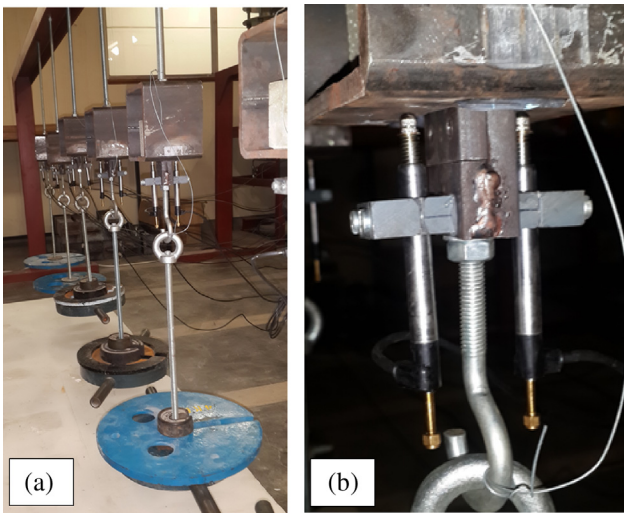

Fig. 5. Pull-out creep test of samples under sustained loadings.

pull-out creep. As noted by Vrijdaghs et al. [32], the pull-out creep would include some measure of fibre slippage from the fibre clamp, which was not determined in this study.

The creep parameters, pull-out rate (*PR*) and the creep coefficient (ϕ^c) for each fibre at 7, 15 and 30 days are presented in Table 3. The computation of these parameters was performed as reported in Abrishambaf et al. [8] as presented in the following equations:

$$PR_{t_2-t_1} = \frac{s_{lt}^{t2} - s_{lt}^{t1}}{t_2 - t_1} \quad (1)$$

$$\phi_{ti}^{C} = \frac{s_{lt}^{ti}}{s_{inst}} \quad (2)$$

where $PR_{t_2-t_1}$ the fibre pull-out rate between time t_2 and t_1, s_{lt}^{ti} represent the pull-out creep at time t_i, ϕ_{ti}^{C}, the pull-out creep coefficient at time t_1 and s_{inst} is the instantaneous fibre slip at loading application.

The results in Table 3 show that the *PR* reduces at later ages for Fibres 1 and 3, while Fibre 2 increases significantly between 7 and 15 days leading to the complete pull-out of the fibre before the 30-day. The creep coefficient, ϕ^c, increases with age but at a decreasing rate.

The significant increase in the s_{lt} of Fibre 2 results from the material property of the fibre. While Fibres 1 and 3 are modified olefin materials, Fibre 2 is a polypropylene fibre, which has a significantly lower elastic modulus as shown in Table 2. Furthermore, Fibres 1 and 3 have embossed surfaces, hence ensuring the penetration of the matrix into the embossment and thereby strengthening the resistance to fibre pull-out. This phenomenon is quite different from that of Fibre 2 without embossment where pull-out resistance is dependent on friction. The increase in the interfacial bond between synthetic fibres and the cement matrix has been shown to be dependent on the surface geometry and material property of the fibre [40].

3.3. Pull-out creep mechanism

As previously pointed out, fibre creep and pull-out have been identified as the two major mechanisms responsible for the time-dependent crack opening of cracked macro-synthetic FRC under sustained load [30,32,41]. A probe into the pull-out phenomena by conducting X-ray CT scans on samples further gives insight into the pull-out mechanism. The results presented in Fig. 8 show the time-dependent pull-out displacements of Fibres 1 and 2,

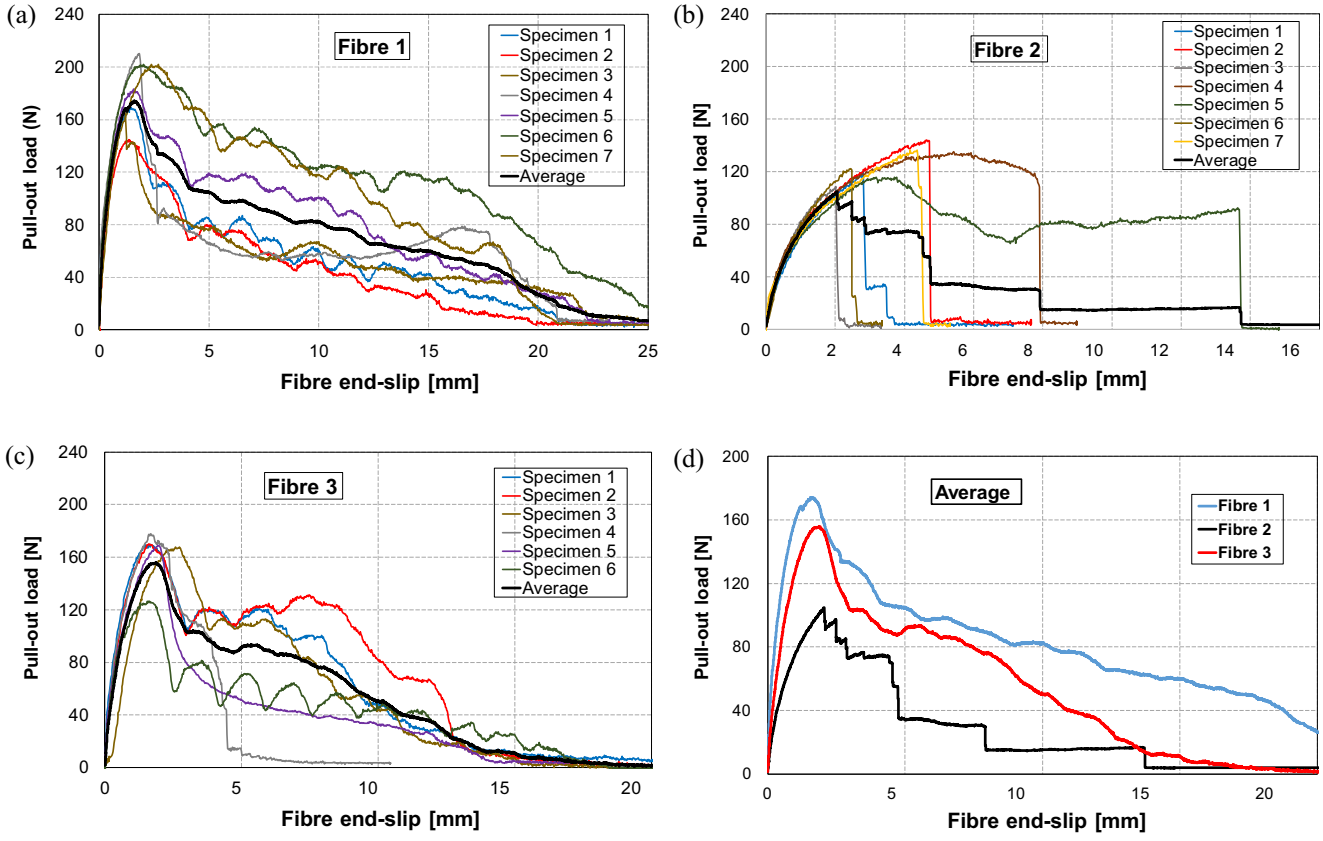

Fig. 6. Pull-out test results, a) Fibre 1, b) Fibre 2, c) Fibre 3 and d) Average fibre responses.

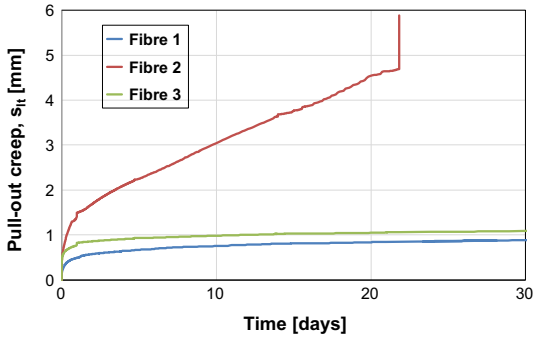

Fig. 7. Pull-out creep response of synthetic macro fibres under sustained loadings.

showing the stages and responses at loading and reloading. It should be noted that the elastic portions have been subtracted. For Fibre 2, after the first unloading and X-ray CT scan were performed, as soon as the sample was reloaded, the fibre fractured. This point has been marked 'X' in Fig. 8b).

The time-dependent fibre slip, s_{lt}, for Fibre 1 at the four stages of unloading (Day 1, 14, 21 and 24) were captured are 0.53, 0.86, 1.27 and 1.50 mm, respectively, while s_{lt} for Fibre 2 is 0.88 mm after 16 h. After each unloading stage, CT scan images were captured to measure the fibre's internal end displacement and the examination of fibre/matrix cross-sectional interface for possible debonding. For the first three stages for Fibre 1, while the LVDT readings have shown some pull-out creep, the CT scan images reveal that the fibre did not experience any internal displacement at the tip (see Fig. 9a & b). No visible sign of debonding is observed at the fibre/-matrix interface close to the fibre end as shown in Fig. 9c).

After the third stage of unloading of Fibre 1, the sample was reloaded to a creep load of 60%. Consequently, fibre pull-out creep was observed in the CT scan images captured after the fourth unloading stage, which is day 24 after test initiation, is shown in Fig. 10. Before subjecting the sample to the CT scan, LVDT measured pull-out creep was 1.50 mm as earlier mentioned, whereas the internal fibre end pull-out was 0.35 mm.

For Fibre 2, only one scan image could be obtained since the fibre fractured after the first scan. Unlike Fibre 1, pull-out creep

Table 3
Pull-out creep parameters of fibres at 50% load level.

Fibre type	δ_{inst} [μm]	Pull-out rate, *PR* [μm/day]			Creep coefficient, ϕ^c		
		(7–0) d	(15–7) d	(30–15) d	(7–0) d	(15–7) d	(30–15) d
Fibre 1	150	65.71	43.75	5.33	3.07	5.40	5.93
Fibre 2	260	187.14	306.25	–	5.04	14.46	–
Fibre 3	250	105.71	36.25	4.67	2.96	4.12	4.40

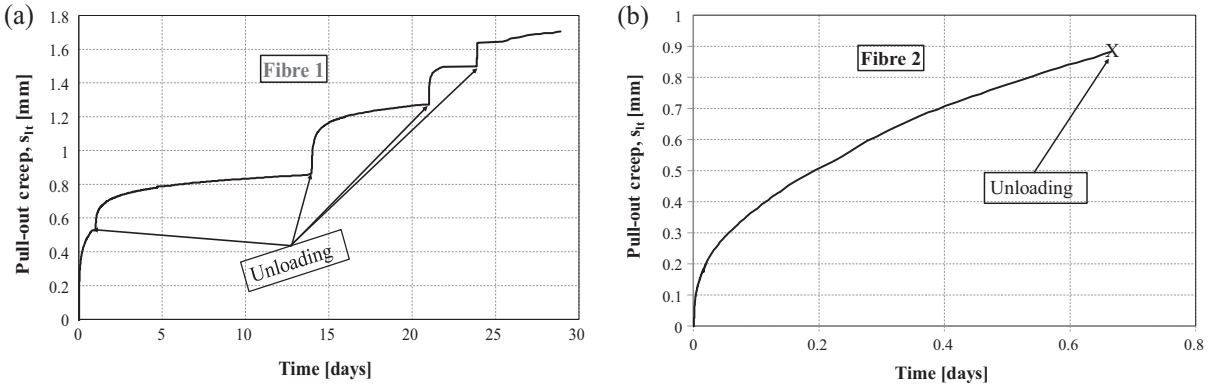

Fig. 8. Pull-out creep response showing different stages of unloading and reloading.

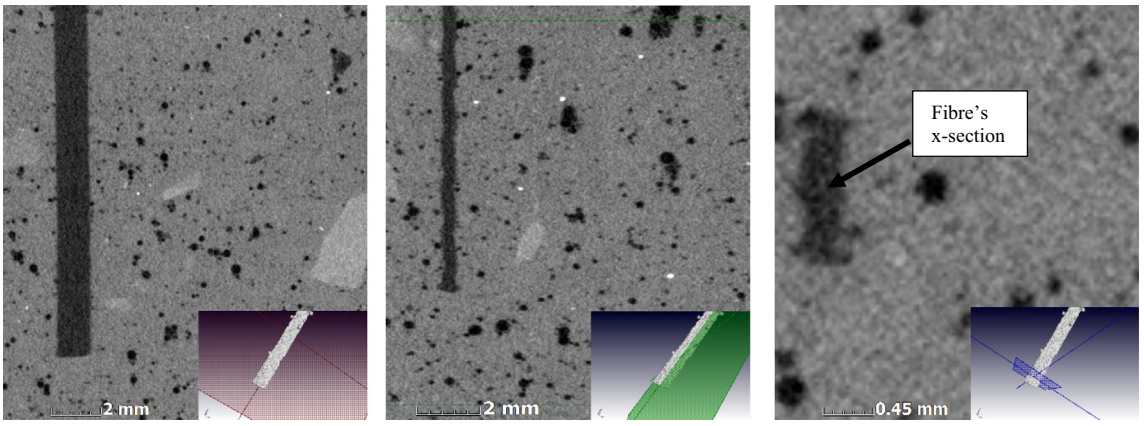

Fig. 9. X-ray CT scan images of sample with Fibre 1 at first three unloading stages.

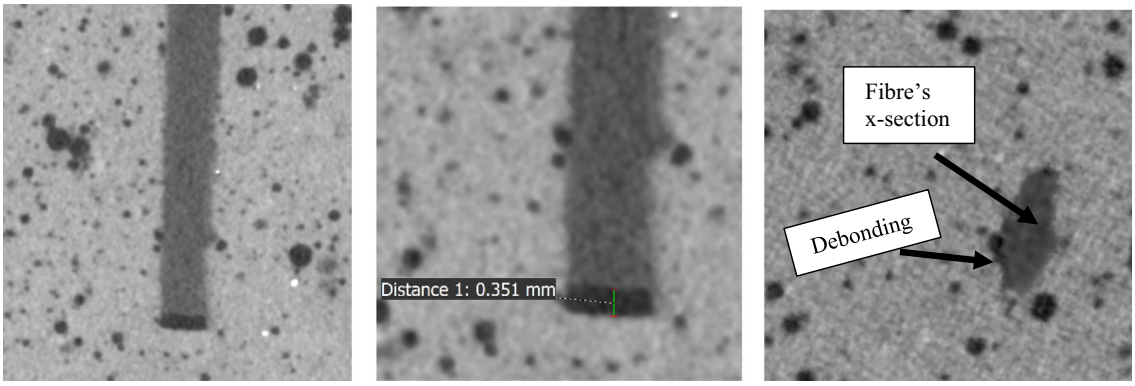

Fig. 10. X-ray CT scan images of sample with Fibre 1 after the fourth unloading stage.

was observed after the first unloading of the test sample at the same period with Fibre 1. The result of the CT scan image is shown in Fig. 11. At the time of unloading, the average LVDT measured pull-out creep was 0.84 mm. However, the measured pull-out creep from the scan image shows a displacement of 0.34 mm.

From the foregoing, it becomes clear that as soon as the creep load is applied to the fibres, an initial debonding occurs around the fibre, few millimetres into the matrix from the fibre entry point. The instantaneous deformation measured (δ_{inst}) reflects the instantaneous elongation of the fibre over the debonded length, rather than an instantaneous fibre pull-out. Fig. 12 shows the debonded region at the fibre entry point and debonding gradually been transferred along the length of the fibre after over 15 days. As noted by Vrijdaghs et al. [32], δ_{inst} is a sum of the instantaneous fibre elongation and the fibre slip in the clamp.

The results presented in Fig. 8 suggest that the fibre creep is the dominant factor in the pull-out creep of synthetic macro fibre. Fig. 9a) shows that no pull-out creep was recorded inside the matrix for Fibre 1 within the first 22 days under sustained load. However, this phenomenon seems to depend on the fibre type/properties, as Fibre 2 already shows pull-out creep within less than a day (Fig. 11). After the fourth stage of reloading of Fibre 1 with an increase in the creep load to 60%, a pull-out creep of the fibre within the sample was recorded (Fig. 10). It follows that the pull-out creep occurred only after full debonding across the length of the fibre and the fibre pulls out be friction. Another possibility is that, the pull-out creep occurred when the bond strength of the fibre/matrix interface around the internal end of the fibre (bonded region) becomes less than the applied stress. This phenomenon is then followed by the time-dependent frictional pull-out of the fibre. As the fibre continuous to gradually pull-out with time, the fibre surface is abraded and coupled with Possion's contraction

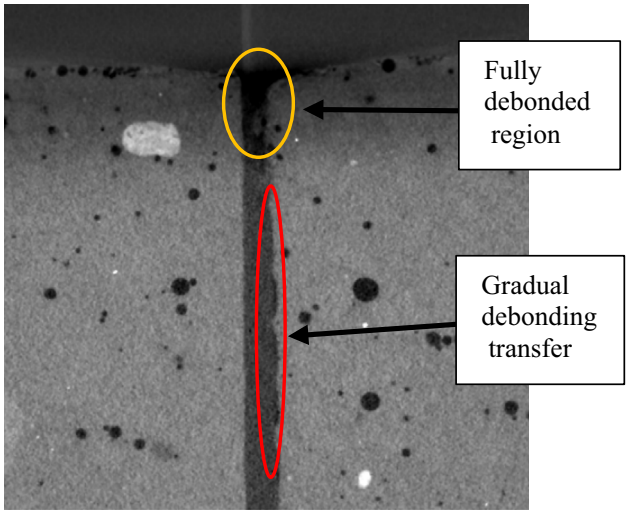

Fig. 12. CT scan image showing debonded region and gradual transfer along fibre length.

[30], a complete loss of bond leading to a sudden fibre pull-out occurs (Fibre 2 in Fig. 7).

One important aspect of this study that needs further investigation is the quantification of the fibre slip within the clamp. While it may be difficult to eliminate such slips when dealing with synthetic fibres, a verified method must be established to quantify the slip. An attempt to quantify this slip with the fibre clamp has been reported in Vrijdaghs et al. [32].

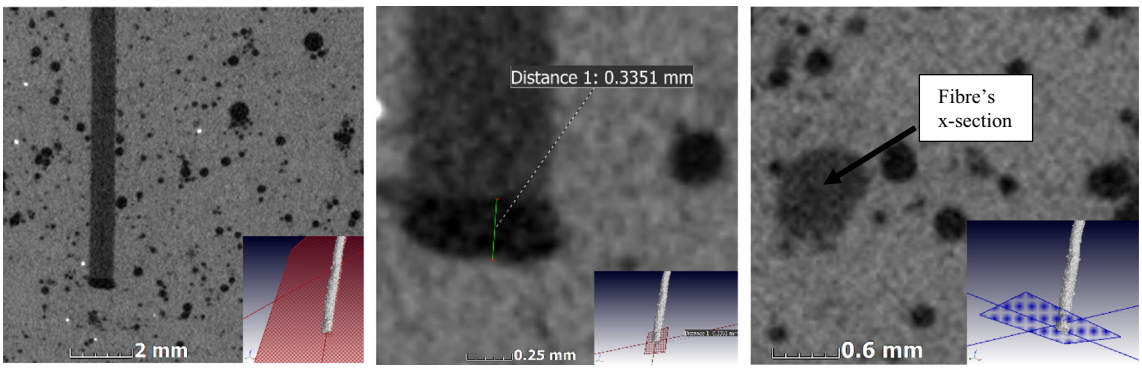

Fig. 11. X-ray CT scan images of sample with Fibre 2 after unloading.

4. Conclusions

A further look into the mechanisms associated with the pull-out creep of synthetic macro fibres under a sustained load has been undertaken. Tests covering instantaneous fibre pull-out, single fibre pull-out creep under sustained loads and X-ray computed tomography scan have been performed and reported in this study. From the findings in this investigation, the following conclusions are drawn.

1. The average maximum pull-out of synthetic macro fibres in a quasi-static test is a function of the fibre type and properties. The better the properties in terms of stiffness, surface configuration and fibre diameter, the better the fibre/matrix interface bond and higher maximum pull-out load.
2. The time-dependent pull-out response of embedded single fibres have also shown to be dependent on the fibre type and properties, with embossed modified olefin fibre showing significantly lesser pull-out creep compared to crimped polypropylene fibre. While the polypropylene fibre pulled out completely without fracturing in 22 days, both modified olefin fibres did not fail at 30 days.
3. The pull-out creep of the polypropylene fibre continued to increase with age, whereas the modified olefin fibres increased at a significantly decreasing rate. Creep rate for the polypropylene fibre was six times more on the 15-day compared to the modified olefin fibre. The increase in the creep coefficient of the modified olefin fibres were not significant even as early as between 15 and 30 days.
4. X-ray computed tomography scan images have revealed that the instantaneous deformation measured soon after the application of creep load if purely the fibre elongation over a debonded area. Depending on the synthetic fibre type/properties, the elongation could take several days before pull-out creep is recorded.
5. While fibre creep and pull-out creep remains the mechanisms for crack opening in macro-synthetic FRC, fibre creep is first initiated under sustained load and then both fibre creep and pull-out creep continues to occurs as the load is sustained until a possible period where failure could occur. However, fibre lengthening is prominent as the pull-out creep shows to be significantly lesser.

Declarations of interest

None.

References

[1] A.M. Brandt, Fibre reinforced cement-based (FRC) composites after over 40 years of development in building and civil engineering, Compos. Struct. 86 (1) (2008) 3–9.
[2] P.D. Nieuwoudt, W.P. Boshoff, Time-dependent pull-out behaviour of hooked-end steel fibres in concrete, Cem. Concr. Compos. 79 (2017) 133–147.
[3] H. Stang, S.P. Shah, Failure of fibre-reinforced composites by pull-out fracture, J. Mater. Sci. 21 (3) (1986) 953–957.
[4] J.A. Barros, V.M. Cunha, A.F. Ribeiro, J.A. Antunes, Post-cracking behaviour of steel fibre reinforced concrete, Mater. Struct. 38 (1) (2005) 47–56.
[5] P. Robins, S. Austin, P. Jones, Pull-out behaviour of hooked steel fibres, Mater. Struct. 35 (7) (2002) 434–442.
[6] V.M. Cunha, J.A. Barros, J.M. Sena-Cruz, Pullout behavior of steel fibers in self-compacting concrete, J. Mater. Civ. Eng. 22 (1) (2009) 1–9.
[7] M.J. Shannag, R. Brincker, W. Hansen, Pullout behavior of steel fibers from cement-based composites, Cem. Concr. Res. 27 (6) (1997) 925–936.
[8] R. Breitenbücher, G. Meschke, F. Song, Y. Zhan, Experimental, analytical and numerical analysis of the pullout behaviour of steel fibres considering different fibre types, inclinations and concrete strengths, Struct. Concr. 15 (2) (2014) 126–135.
[9] A. Abrishambaf, J.A. Barros, V.M. Cunha, C. Frazão, Time-dependent behaviour of fibre pull-out in self-compacting concrete, Cem. Concr. Compos. 77 (2017) 14–28.
[10] E. Zile, O. Zile, Effect of the fiber geometry on the pullout response of mechanically deformed steel fibers, Cem. Concr. Res. 44 (2013) 18–24.
[11] A. Beglarigale, H. Yazıcı, Pull-out behavior of steel fiber embedded in flowable RPC and ordinary mortar, Constr. Build. Mater. 75 (2015) 255–265.
[12] A. Beglarigale, S. Aydin, C. Kizilirmak, Fiber-matrix bond characteristics of alkali-activated slag cement-based composites, J. Mater. Civ. Eng. 28 (11) (2016) 04016133, https://doi.org/10.1061/(ASCE)MT.1943-5533.0001642.
[13] A. Khabaz, Performance evaluation of corrugated steel fiber in cementitious matrix, Constr. Build. Mater. 128 (2016) 373–383.
[14] F. Laranjeira, C. Molins, A. Aguado, Predicting the pullout response of inclined hooked steel fibers, Cem. Concr. Res. 40 (10) (2010) 1471–1487.
[15] A.J. Babafemi, W.P. Boshoff, Pull-out response of macro synthetic fibre from concrete matrix: effect of loading rate and embedment length, Constr. Build. Mater. 135 (2017) 590–599.
[16] W.P. Boshoff, V. Mechtcherine, G.P. van Zijl, Characterising the time-dependant behaviour on the single fibre level of SHCC: Part 2: the rate effects on fibre pull-out tests, Cem. Concr. Res. 39 (9) (2009) 787–797.
[17] J. MacKay, J.F. Trottier, Post-crack creep behavior of steel and synthetic FRC under flexural loading, in: Shotcrete: More Engineering Developments, 2004, pp. 183–192.
[18] B.H. Oh, J.C. Kim, Y.C. Choi, Fracture behavior of concrete members reinforced with structural synthetic fibers, Eng. Fract. Mech. 74 (1) (2007) 243–257.
[19] N. Buratti, C. Mazzotti, M. Savoia, Post-cracking behaviour of steel and macro-synthetic fibre-reinforced concretes, Constr. Build. Mater. 25 (5) (2011) 2713–2722.
[20] M.N. Soutsos, T.T. Le, A.P. Lampropoulos, Flexural performance of fibre reinforced concrete made with steel and synthetic fibres, Constr. Build. Mater. 36 (2012) 704–710.
[21] A.M. Alani, D. Beckett, Mechanical properties of a large-scale synthetic fibre reinforced concrete ground slab, Constr. Build. Mater. 41 (2013) 335–344.
[22] P. Pujadas, A. Blanco, S. Cavalaro, A. de la Fuente, A. Aguado, Fibre distribution in macro-plastic fibre reinforced concrete slab-panels, Constr. Build. Mater. 64 (2014) 496–503.
[23] V.C. Li, Y. Wang, S. Backer, Effect of inclining angle, bundling and surface treatment on synthetic fibre pull-out from a cement matrix, Composites 21 (2) (1990) 132–140.
[24] H.S. Armelin, N. Banthia, Predicting the flexural postcracking performance of steel fiber reinforced concrete from the pullout of single fibers, ACI Mater. J. 94 (1) (1997) 18–31.
[25] S. Singh, A. Shukla, R. Brown, Pullout behavior of polypropylene fibers from cementitious matrix, Cem. Concr. Res. 34 (10) (2004) 1919–1925.
[26] A.E. Richardson, Bond characteristics of structural polypropylene fibres in concrete with regards to post-crack strength and durable design, Struct. Surv. 23 (3) (2005) 210–230.
[27] J.P. Won, D.H. Lim, C.G. Park, Bond behaviour and flexural performance of structural synthetic fibre-reinforced concrete, Mag. Concr. Res. 58 (6) (2006) 401–410.
[28] H.R. Pakravan, M. Jamshidi, M. Latifi, Polymeric fibers pullout behavior and microstructure as cementitious composites reinforcement, J. Text. Inst. 104 (10) (2013) 1056–1064.
[29] P. Di Maida, E. Radi, C. Sciancalepore, F. Bondioli, Pullout behavior of polypropylene macro-synthetic fibers treated with nano-silica, Constr. Build. Mater. 82 (2015) 39–44.
[30] A.J. Babafemi, W.P. Boshoff, Tensile creep of macro-synthetic fibre reinforced concrete (MSFRC) under uni-axial tensile loading, Cem. Concr. Compos. 55 (2015) 62–69.
[31] W.P. Boshoff, V. Mechtcherine, G.P. van Zijl, Characterising the time-dependant behaviour on the single fibre level of SHCC: Part 1: mechanism of fibre pull-out creep, Cem. Concr. Res. 39 (9) (2009) 779–786.
[32] R. Vrijdaghs, M. di Prisco, L. Vandewalle, Short-term and creep pull-out behavior of polypropylene macrofibers at varying embedded lengths and angles from a concrete matrix, Constr. Build. Mater. 147 (2017) 858–864.
[33] E. Maire, P.J. Withers, Quantitative X-ray tomography, Int. Mater. Rev. 59 (1) (2014) 1–43.
[34] A. Du Plessis, B.J. Olawuyi, W.P. Boshoff, S.G. Le Roux, Simple and fast porosity analysis of concrete using X-ray computed tomography, Mater. Struct. 49 (1–2) (2016) 553–562.
[35] EN12350-2, Testing Fresh Concrete - Slump Test, British Standards Institution, London, 2000.
[36] EN 14889-2, Fibres for Concrete. Polymer Fibres. Definitions, Specifications and Conformity, British Standard Institution, London, 2006.
[37] J.O. Lerch, H.L. Bester, A.S. Van Rooyen, R. Combrinck, W.I. de Villiers, W.P. Boshoff, The effect of mixing on the performance of macro synthetic fibre reinforced concrete, Cem. Concr. Res. 103 (2018) 130–139.
[38] EN12390-3, Testing Hardened Concrete – Compressive Strength of Test Specimens, British Standards Institution, London, 2002.
[39] A. du Plessis, S.G. le Roux, A. Guelpa, The CT Scanner Facility at Stellenbosch University: an open access X-ray computed tomography laboratory, Nucl. Instr. Meth. B 384 (2016) 42–49.
[40] S. Singh, A. Shukla, R. Brown, Pull-out behaviour of polypropylene fibres from cementitious matrix, Cem. Concr. Res. 34 (2004) 1919–1925.
[41] E.S. Bernard, Creep of Cracked fibre reinforced shotcrete panels, in: Shotcrete: More Engineering Developments, 2004, pp. 47–57.